

(2) Subsequent heating due to sequential solidification of droplets does not apply to our studies of the as-splatted condition because we did not observe surface precipitation, which is characteristic of decomposition on annealing splat quenched specimens (Scott and Leake [6]) and supersaturated thin foils in general [7]. A similar argument may be used to reject heating during ion beam thinning which in our experience normally arises from incorrect selection, and/or inadequate control of thinning conditions and/or poor thermal contact with support materials. Control specimens of quenched supersaturated Al-4%Cu alloys did not decompose as a result of ion beam thinning under identical conditions.

In conclusion it is obvious that interpretation of splat quenched microstructures is not straightforward in view of the many possible variables affecting the formation of the microstructure, and the lack of independent measurement of the variables that may control the solidification and precipitation processes at different points in the specimen. Our original use of a microstructural standard was an attempt to bring some degree of rationality to the issue. Obviously if the assumptions inherent in our standardization are not operating, then different factors will affect the observed microstructure. This observation was assumed to be trivial. We feel strongly that our method of determining the principal factors

affecting the microstructure is still the only rational way available at present to permit comparison of microstructures from different splatted specimens, and different regions of the same splat.

## References

1. M. G. SCOTT, M. KJEK and H. MATYA, *J. Mater. Sci.* **13** (1978) 1354.
2. D. B. WILLIAMS and J. W. EDINGTON, *ibid.* **11** (1976) 2146.
3. *Idem, ibid.* **11** (1976) 2151.
4. *Idem, ibid.* **12** (1977) 126.
5. J. M. VITEK, *ibid.* **10** (1975) 1828.
6. M. G. SCOTT and J. A. LEAKE, *Acta Met.* **23** (1975) 2153.
7. K. C. THOMPSON-RUSSELL and J. W. EDINGTON, "Electron Microscope Specimen Preparation Techniques in Materials Science" (Macmillan, London, 1977) p. 15.

*Received and accepted 16 January 1978.*

D. B. WILLIAMS  
*Department of Metallurgy and Materials  
 Engineering,  
 Lehigh University,  
 Bethlehem, Pennsylvania 18015, USA*

J. W. EDINGTON  
*Department of Mechanical and Aerospace  
 Engineering,  
 University of Delaware,  
 Newark, Delaware 19711, USA*

## *Cyclic fatigue of polycrystalline alumina in direct push-pull*

Whilst considerable effort has been made in the study of fracture strength and creep properties of ceramic materials, comparatively little is known about their behaviour under cyclic fatigue conditions. Dynamic fatigue testing of brittle materials seems to be a difficult problem and in those few cases where it has been attempted it has yielded a wide scatter in the data, so that statistical methods of analysis have had to be employed [1-2].

More recently a limited amount of data has become available [3] on mechanical fatigue of Al<sub>2</sub>O<sub>3</sub> which seems to show that this material is susceptible to dynamic fatigue. These results were obtained in repeated *uni-directional bending*, and

as far as can be ascertained the influence of cyclic tension compression on fatigue behaviour of ceramics has never before been investigated. A method of dynamic fatigue testing of brittle materials in direct push-pull is described in this note. The method has been successfully applied to fatigue testing of "Lucalox" alumina.

The fatigue tests were carried out in a "Mayes" servohydraulic testing machine equipped with a low capacity pump for smooth running up to frequencies of 10 Hz. The use of a hydraulic machine is important to ensure axial movement of the loading ram. The gripping fixture consists simply of two adaptors (one mounted on the moving ram, the other on the load cell) each one containing a standard "Marlco" friction spring collet. The specimens, with cylindrical shoulders, are thus

held tightly in the collets by friction forces. A capacitance displacement transducer was fitted at the ends of the sample. This not only measured strain, but also served the purpose of indicating instantaneously whether there was any slip in the specimen grip during the fatigue test at constant load amplitude. An essential requirement for the success of this technique is an extremely good axial alignment of the gripping system and accurate machining of the specimens. The spring collets were aligned prior to each test using a long straight alumina rod accurately machined and especially prepared for this purpose. The method of specimen preparation is described below.

The specimens used had cylindrical shape with a total length of 1.25 in and a reduced gauge of 0.5 in at the centre. The straight middle part of the gauge length had a diameter of 3 mm. The diameter of the shoulders was either  $\frac{7}{32}$  in or 0.5 mm in order to fit the size of standard collets. The tolerance in these dimensions was  $\pm 0.005$  mm. The material used for the present investigation was single phase polycrystalline alumina (Lucalox) obtained as rods from General Electric (USA). The material was translucent, of 99.9% purity and of about 99.5% of the theoretical density. The average grain size had a variation of 13 to 30  $\mu\text{m}$  from rod to rod.

These rods were available in variable lengths and with a diameter between  $\frac{1}{4}$  and  $\frac{7}{32}$  in, and the specimens were machined as follows. The ends of the rods were inserted and glued to cylindrical mild steel caps with accurately aligned "false centres" machined in them. They were then set in a cylindrical grinding machine, between carbide tipped centres and ground with a diamond wheel (lubricated with a solution of anti-corrosive in water) turning at a peripheral speed of 3900  $\text{cm sec}^{-1}$  and ground at an infeed of  $2.5 \times 10^{-4}$  cm per pass. The whole length of the rod was ground to the final diameter of the shoulders. The gauge length of the specimen was then ground with a wheel which had the gauge profile. One, two, or three gauge lengths were ground along the rod (to obtain, one, two or three specimens) depending on the initial length of the rod. If this rod was long enough to obtain 3 specimens, or more, it was held against alumina steadies on either side of the gauge length being machined and on the opposite side of the rod to the grinding wheel. The specimen was

thus prevented of bowing against the wheel when it became thinner in the central portion.

The bowing limits of the finished specimens were measured by rotating between two precision dial gauges ("Mikrokator" C.E. Johansson Ltd.), and gave a consistent measurement to within  $\pm 1.0 \times 10^{-4}$  cm. It is known from previous experience [4] that this is within the permissible deviation from straightness to avoid excessive bending of the specimen when subjected to axial loading. A view of the finished specimens is shown in Fig. 1.

The surface finish of the gauge length was measured on a "Tallysurf". Occasional depressions of 4  $\mu\text{m}$  are observed which correspond to approximately one fifth of a mean grain diameter. The surface of the machined sample was also observed under the SEM after having evaporated a gold layer on it. A view of this surface is shown in Fig. 2. It can be seen that there are some "holes", or deep scratches, on the surface, probably the result of grain pull-out. The largest size hole observed was about  $3 \times 6 \mu\text{m}$ , or  $\frac{1}{3}$  to  $\frac{1}{4}$  of the average grain size, although the depth of the hole cannot be estimated by this method. After machining the specimens were rinsed in water and dried in an oven.

Two types of tests were conducted with the alumina samples machined as described above: cyclic push-pull at a frequency of 5 Hz, at constant load amplitude, using a sine waveform, and constant load tests. In both cases the specimens

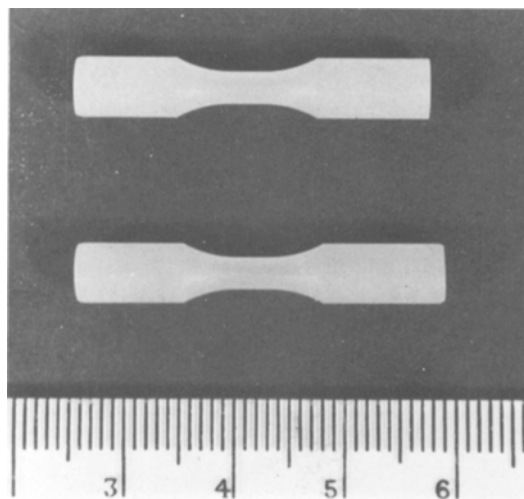


Figure 1 Shape and size of the machined alumina samples.

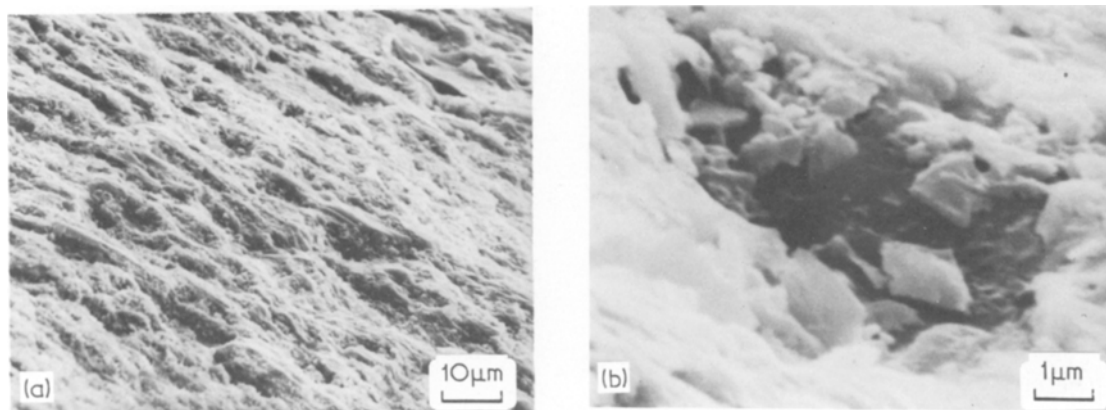


Figure 2 Scanning electron micrograph of the machined surface of a specimen shown at two magnifications.

were tested to fracture whilst the number of cycles and time to fracture were measured. The final load for both cyclic or constant stressing was not applied to the sample from the very first instant of the test, but was built up slowly from a low value to prevent shock loading. The rate of build-up was such that it took 20 sec to reach the full load.

The tests were conducted at ordinary temperature and environment where the relative humidity was about 70%. The results of these tests are shown in Fig. 3 as a plot of stress against both number of cycles and time to fracture. Three curves are shown in this figure. The results of curves 1 and 2 were obtained with samples machined from three different rods which were used indiscriminately for cyclic tests and constant load tests. There is little scatter in these results,

which shows that the samples take a longer time to fracture if they are under constant stress. The results of curve 3 were all obtained with specimens machined from a different rod. The times to fracture under constant load for these specimens are longer than for any of the other samples. It was thought that this particular rod was intrinsically stronger than any of the others tested, and in order to check this, a sample from this rod was tested under cyclic loading. This gave the result represented by point A in the figure showing that even in stress cycling this sample had a higher fatigue strength than any other.

In order to detect any possible differences between the rods which yielded these different results, scanning electron micrographs were taken of the fractured surfaces of samples from curves

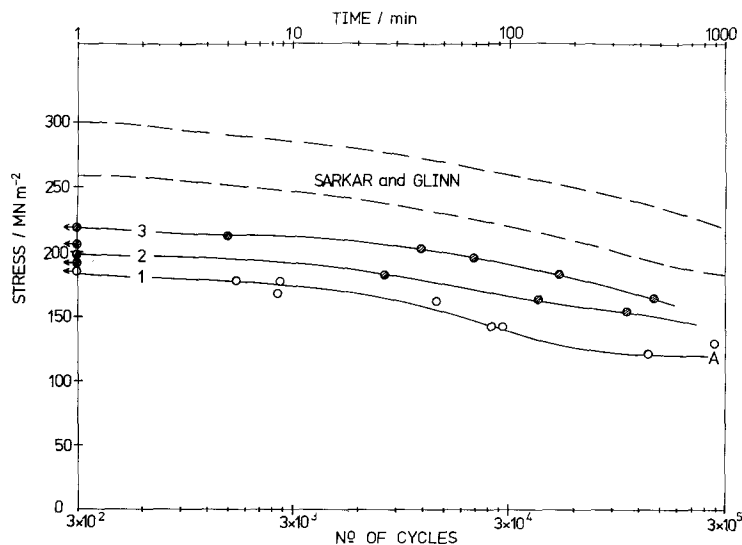


Figure 3 Peak stress, or constant stress, against both the number of cycles to fracture and time to fracture. Curve 1 is the cyclic fatigue curve. Curves 2 and 3 are static fatigue curves.

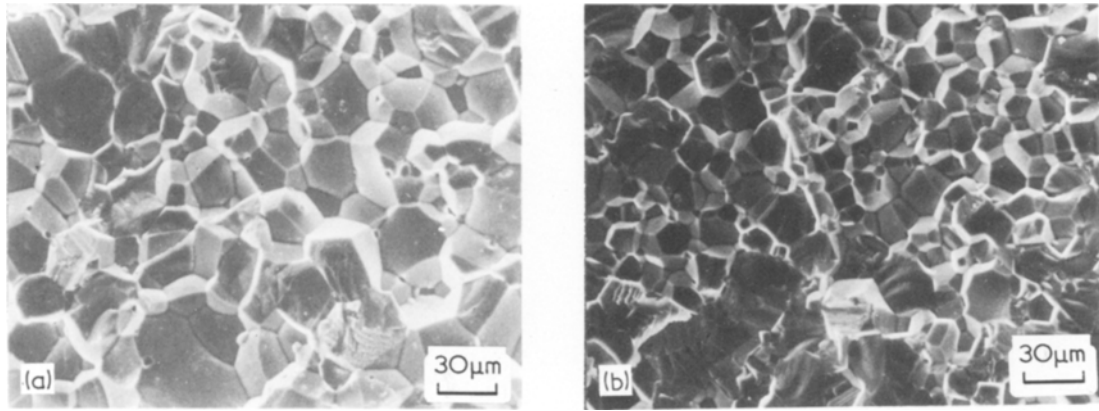


Figure 4 Scanning electron micrographs of the fracture surface of typical samples of (a) curve 2, and (b) curve 3 of Fig. 3.

1, 2 and 3. Typical micrographs are shown in Fig. 4. It is clear that the stronger specimens have a smaller grain size (average  $\approx 18 \mu\text{m}$ , maximum  $\approx 35 \mu\text{m}$ ) than the specimens of curves 1 and 2 (average grain size  $\approx 29 \mu\text{m}$ ; maximum grain size  $\approx 60 \mu\text{m}$ ). Some small pores can also be seen in the latter material whilst no pores were visible in the stronger samples. The difference in the results can therefore be satisfactorily explained by the difference in structure.

The points shown in Fig. 3 for fracture times of 1 min correspond really to samples broken at the end of the load build-up and they should therefore be considered as values of the tensile strength at the particular rate of loading used.

It seems that this method of testing produces results which are highly reproducible, the scatter of points being so small that a  $\sigma-N$  fatigue curve can be very accurately drawn. This curve has the same shape as that obtained by Sarkar and Glinn [3], with much greater scatter, in their cyclic fatigue tests performed in bending, although the  $\sigma-N$  curve of Fig. 3 is shifted downwards to lower stresses.

The influence of cyclic loading on fatigue life is also apparent. Specimens stressed at constant load took a much longer time to fracture. This difference is accentuated by the fact that the cyclically stressed samples were under tensile load only for half of the time to fracture. It is therefore impossible to explain the results of dynamic cyclic fatigue by a mechanism of crack growth similar to that which controls the static fatigue time to failure such as environmental stress corrosion alone [5]. These results seem to

support the view that some type of "deformation damage" occurs during cyclic fatigue testing of  $\text{Al}_2\text{O}_3$  [6].

The tensile strength of the alumina tested is given by the points in the graph (Fig. 3) corresponding to 1 min time to fracture. Even the scatter in these points is small, the fracture strength for specimens of curves 1 and 2 being  $(195 \pm 10) \text{MNm}^{-2}$ , which is agreement with the values quoted by other authors [7, 8] for polycrystalline alumina of 99.5% and  $50 \mu\text{m}$  grain size. From the value quoted for the effective surface energy of pure  $\text{Al}_2\text{O}_3$  ( $\gamma_I = 24 \text{Jm}^{-2}$ ) [7] it should be possible to obtain an estimate of the critical flaw, or crack, size for fracture at the various stress levels using the generalized Griffith expression

$$\sigma = \frac{1}{Y} \left( \frac{2E \gamma_I}{c} \right)^{1/2}$$

for the fracture stress  $\sigma$ , where  $c$  is crack length and  $E$  is Young's modulus. In this equation  $Y$  is a factor which depends on specimen geometry and size, but unfortunately no exact values of  $Y$  exist for the specimen geometry used in the present tests. It is useful however to obtain a crude estimate taking

$$\frac{1}{Y} = \left( \frac{\pi}{4(1-\nu^2)} \right)^{1/2} \approx 0.93 \quad (\nu = \text{Poisson's ratio})$$

as for the case of a circular crack in an infinite medium [9]. This gives the relationship

$$\sigma^2 c = 15.6$$

between the fracture stress and crack size. Using

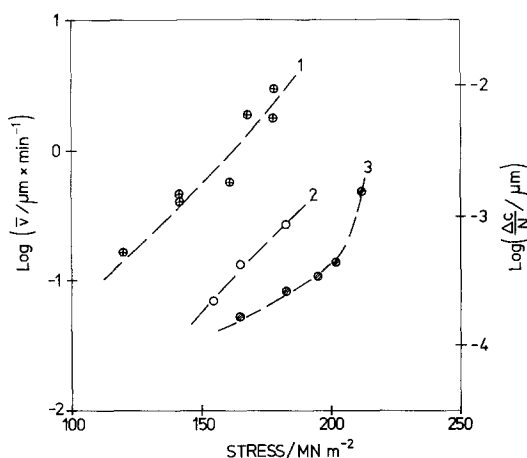


Figure 5 Peak stress, or constant stress, against logarithm of crack growth rate, and logarithm of crack velocity.

the experimental values  $\sigma_0 = 195 \text{ MN m}^{-2}$  and  $\sigma_0 = 218 \text{ MN m}^{-2}$  for the tensile strength of the "weak" and "strong" material respectively the initial flaw sizes  $c_0 = 41 \mu\text{m}$  and  $c_0 = 33 \mu\text{m}$  are obtained. These seem to be reasonable values, since they are nearly equal to the size of the largest grains.

The time to fracture,  $\Delta t$ , or the number of cycles to fracture,  $N$ , can be interpreted as the time, or cycles, taken for the cracks to grow from the initial size  $c_0$  to the critical size,  $c_0 + \Delta c$ , under the applied stress conditions. The ratio  $\Delta c/\Delta t$ , or  $\Delta c/N$ , can be taken as a measure of the "gross average" crack velocity, or crack growth rate. Values of  $\log(\Delta c/\Delta t)$  and  $\log(\Delta c/N)$  have been calculated using the data of curves 1, 2 and 3 of Fig. 3 and plotted against maximum stress in Fig. 5. Since the crack velocity is usually related to the stress intensity factor  $K_I$  through a power function, such as  $V = AK_I^n$ , the "gross average" crack velocity is not a particularly meaningful parameter. It is used here only to show clearly and consistently how the crack velocity increases with

stress and that for a given maximum stress value this velocity is in cyclic fatigue about 10 times greater than under static loading conditions.

It can therefore be concluded that the method of cyclic fatigue testing developed has been successfully applied to polycrystalline alumina and it has been shown that in this material cracks propagate faster under cyclic loads than under constant load conditions. This result suggests that alumina is susceptible to mechanical fatigue damage.

### Acknowledgements

The author wishes to thank Mr A. Buckingham for his assistance with the machining of the specimens, the S.R.C. for financial support, and the C.R.F. of London University for an equipment grant.

### References

1. D. A. KROHN and D. P. H. HASSELMAN, *J. Amer. Ceram. Soc.*, **55** (1972) 280.
2. C. P. CHEN and W. J. KNAPP, "Fracture Mechanics of Ceramics" (Plenum Press, 1973) p. 691.
3. B. K. SARKAR and T. G. T. GLINN, *Trans. Brit. Ceram. Soc.* **69** (1970) 199.
4. S. K. SINHA RAY, Ph.D. Thesis, University of London (1972).
5. A. G. EVANS and E. R. FULLER, *Metall. Trans.* **5** (1974) 27.
6. S. L. WILLIAMS, "Mechanical Properties of Engineering Ceramics", edited by W. Kriegel and H. Palmour (Interscience, 1961) p. 245.
7. R. W. DAVIDGE and G. TAPPIN, *Proc. Brit. Ceram. Soc.* **15** (1970) 47.
8. R. W. DAVIDGE and A. G. EVANS, *Mater. Sci. Eng.* **6** (1970) 281.
9. I. N. SNEDDON, *Proc. Roy. Soc.* **A187** (1946) 229.

Received 9 August

and accepted 19 October 1977.

F. GUIU

Department of Materials,  
Queen Mary College,  
London, UK

### Cathodoluminescence from slip planes in deformed MgO

Dislocations and their associated atmospheres of impurities or other point defects influence locally the luminescent properties of some ionic and semiconductor crystals as GaP [1] CdS [2] and GaAs [3, 4]. To investigate such influence the

SEM in the cathodoluminescence mode has been frequently applied.

The effect of dislocations luminescence has been sometimes studied on plastically deformed crystals [5, 6] and the traces of slip planes in GaP [7] have been observed in the cathodoluminescence image. In the case of MgO crystals, it has been found [8, 9] that a concentrated load produced